

A High-throughput Quantitative Multiplex Kinase Assay for Monitoring Information Flow in Signaling Networks

APPLICATION TO SEPSIS-APOPTOSIS*

Kevin A. Janes‡, John G. Albeck§, Lili X. Peng‡, Peter K. Sorger‡§¶, Douglas A. Lauffenburger‡§¶, and Michael B. Yaffe‡§¶||

To treat complex human diseases effectively, a systems-level approach is needed to understand the interplay of environmental cues, intracellular signals, and cellular behaviors that underlie disease states. This approach requires high-throughput, multiplex techniques that measure quantitative temporal variations of multiple protein activities in the intracellular signaling network. Here, we describe a single microtiter-based format that simultaneously quantifies protein kinase activities in the phosphatidylinositol 3-kinase pathway (Akt), nuclear factor- κ B pathway (IKK), and three core mitogen-activated protein kinase pathways (ERK, JNK1, MK2). These parallel high-throughput assays are stringently linear, redundantly specific, reproducible, and sensitive compared with classical low-throughput techniques. When applied to a model of sepsis-induced colon epithelial apoptosis, this approach identified a late phase of Akt activity as a critical mediator of cell survival that quantitatively contributed to the efficacy of insulin as an anti-apoptotic cue. Thus, sampling parallel nodes in the intracellular signaling network identified part of the molecular mechanism underlying the efficacy of insulin in the treatment of human sepsis. *Molecular & Cellular Proteomics* 2:463–473, 2003.

Complex patterns of signal transduction arise when cells are exposed to combinations of extracellular cues that vary in onset, duration, origin, and synchrony. Cells process these cues through an interconnected network of multifunctional, redundant molecules to elicit a set of phenotypic responses that subsequently impact function at the cell, tissue, and organ level. In order to develop a molecular understanding of the complex pathophysiology underlying human diseases and utilize this information for prognosis and therapy, a systems-level, network-biology approach should be applied to the signaling networks governing the relevant cell responses (1). This approach will require frequent temporal sampling of pro-

tein activity at critical nodes within parallel signaling pathways inside the cell in a quantitative manner to characterize the flow of information accurately. Such functional measurements are likely to be as valuable, or more valuable, than measurements of simple protein abundance. By quantitatively exploring the functional response of the signaling network to distinct extracellular cues and correlating these molecular events with phenotypic responses, one can construct predictive models of cue-signal and signal-response relationships.

Evolving proteomic approaches to network biology have largely focused on measuring abundances of many proteins at only a few time points or under a limited number of experimental conditions (2). Complementary information on functional protein characteristics, such as enzyme activity, has been lacking in these systematic analyses, in large part because there do not exist quantitatively robust, high-throughput techniques that simultaneously measure multiple protein activities in cells. Initially, this type of data collection on protein functional status should focus on frequent sampling of a limited number of key molecules that sit at critical nodes in different signaling pathways (Fig. 1A).

To begin to address this, we have developed a generalized assay for the multiplex analysis of multiple protein kinase activities in a 96-well format. The procedure utilizes parallel kinase-specific immunopurification steps, followed by rapid quantitative high-throughput activity measurements within the linear-rate regime for each kinase. We applied this technique to measure the activities of five kinases (extracellular-regulated kinase (ERK)¹ (3), Akt, I κ -B kinase (IKK), c-jun N-terminal kinase 1 (JNK1), and mitogen-activated protein kinase-associated protein kinase 2 (MK2)) in a sepsis/systemic inflammatory response syndrome (SIRS) model system for tumor necrosis factor-alpha (TNF- α)-induced colon epithelial cell death.

¹ The abbreviations used are: ERK, extracellular-regulated kinase; IKK, I κ -B kinase; JNK1, c-jun N-terminal kinase 1; MK2, mitogen-activated protein kinase-associated protein kinase 2; PC, phosphocellulose; PI 3-K, phosphatidylinositol 3-kinase; SIRS, systemic inflammatory response syndrome; TNF- α , tumor necrosis factor-alpha; DTT, dithiothreitol; IFN- γ , interferon gamma; GST, glutathione S-transferase; CPM, counts per minute.

From the ‡Biological Engineering Division, §Department of Biology, and ¶Center for Cancer Research, Massachusetts Institute of Technology, 400 Main Street, Cambridge, MA 02139

Received, May 16, 2003, and in revised form, June 25, 2003

Published, MCP Papers in Press, June 26, 2003, DOI 10.1074/mcp.M300045-MCP200

We chose this experimental model because, clinically, sepsis is the most common cause of death in critically ill patients and is a prime example of acute, systemic disease mediated by molecular network dysfunction (4, 5). Despite the multifaceted etiology of sepsis, the colonic epithelium represents a common final effector organ and is a major site for programmed cell death following injury (6). Epithelial apoptosis is believed to cause gut barrier dysfunction (7), leading to leakage of cytokines and possibly bacteria into the systemic circulation, thereby exacerbating the inflammatory state. Thus, the bowel has been postulated to be the “motor” driving the septic state (8). TNF- α levels are drastically elevated in a number of forms of human sepsis, and levels correlate with increased mortality (9). The five kinases whose activities we measured function downstream of TNF- α as canonical hubs for signaling pathways that control cell survival, stress responses, and the onset of programmed cell death (Fig. 1A, gray nodes) (10–13). Quantitative sampling of the activity of these kinases in time with the high-throughput multiplex assays provided a window into the state of the signaling network in this model of cytokine-induced human disease.

Due to the complexity of the disease, treatments for sepsis have proven elusive, with certain monotherapies (e.g. TNF antagonists (14)) actually worsening patient survival. Intriguingly, intensive insulin therapy has recently been found to reduce morbidity in critical illness substantially (15), though the mechanism underlying this effect is unknown (4). A number of possibilities have been proposed, including tight regulation of glucose levels (16), antagonism of proinflammatory molecules (17), and reduction of circulating C-reactive protein levels (18).

At the molecular level, TNF- α and insulin activate a number of common signaling pathways that are highly interconnected (Fig. 1A), and it is difficult to predict *a priori* how these conflicting cues are processed intracellularly to determine cell fate in physiologically relevant cell types. We hypothesized that quantitative, dynamic measurement of information flow through these critical signaling nodes might clarify how network information is processed and reveal new signal-response relationships involving insulin’s mechanism of action in sepsis.

We implemented an *in vitro* model of TNF-induced programmed cell death in a human colon epithelial cell line that survives TNF- α treatment when costimulated with insulin. The network response to TNF- α and insulin as combinatorial cues in this model system was then explored by performing over 400 independent kinase activity measurements with the high-throughput assays. A significant reduction in TNF-induced colon epithelial death was observed upon insulin treatment. This correlated with a profound change in the pattern of Akt kinase activity, with only minor perturbations observed in the activities of other kinases that were assayed. We were able to attribute at least half of the insulin-induced survival effect to the specific activation of the Akt pathway at late times. Im-

portantly, we found that the addition of insulin 4 h after TNF- α addition provided sufficient late-phase Akt activity to elicit the same survival effect as when insulin was added simultaneously with TNF- α , suggesting a molecular mechanism for how insulin improves patient survival in sepsis even when administered hours after the initial insult. The assay format and approach that we report here provides a common platform that can now be used to systematically probe multiple signal transduction pathways at moderate sampling rates under diverse experimental conditions of broad scientific and medical interest.

EXPERIMENTAL PROCEDURES

Cell Culture, Stimulation, and Lysis—HT-29 and HeLa cells (ATCC, Manassas, VA) were grown according to the manufacturer’s recommendations. For the time courses, HT-29 cells were seeded at 50,000 cells/cm², grown for 24 h, and then treated with 200 U/ml IFN- γ (Roche) for an additional 24 h. After sensitization, cells were rinsed once with PBS and treated with 50 ng/ml TNF- α (Peprotech, Rocky Hill, NJ) with or without 100 nM insulin (Sigma) for the indicated times. Cells were washed once with ice-cold PBS and lysed in 1% Triton X-100, 50 mM Tris-HCl (pH 7.5), 150 mM NaCl, 50 mM β -glycerophosphate, 10 mM sodium pyrophosphate, 30 mM NaF, 1 mM benzamidine, 2 mM EGTA, 100 μ M NaVO₄, 1 mM dithiothreitol (DTT), 1 mM phenylmethylsulfonyl fluoride, 10 μ g/ml aprotinin, 10 μ g/ml leupeptin, 1 μ g/ml pepstatin, 1 μ g/ml microcystin-LR. Whole cell lysates were incubated on ice for 15 min, then clarified by centrifugation at 16,000 $\times g$ for 15 min at 4 °C. Protein concentrations of clarified extracts were determined with a bicinchoninic acid assay (Pierce).

High-throughput Kinase Activity Assays—The microtiter-based kinase activity assays were performed with the following antibodies: anti-ERK1/2 CT (Upstate Biotechnology, Lake Placid, NY), anti-Akt PH domain (Upstate Biotechnology), anti-JNK1 (Santa Cruz Biotechnology, Santa Cruz, CA), anti-IKK α/β (Santa Cruz Biotechnology) or anti-MK2 (Upstate Biotechnology). Protein A or G microtiter strips (Pierce) were coated overnight with 10 μ g/ml anti-kinase antibody and washed three times with blocking buffer (1% bovine serum albumin (Sigma) in 50 mM Tris-HCl (pH 7.5), 150 mM NaCl, 0.05% Triton X-100). Cell lysates (50 μ g for ERK, 500 μ g for Akt, 200 μ g for JNK1, 200 μ g for MK2, 600 μ g for IKK) were added for 3 h (ERK, Akt, JNK1, and MK2) or overnight (IKK), then washed two times with wash buffer (50 mM Tris-HCl (pH 7.5), 150 mM NaCl) and two times with kinase wash buffer (20 mM Tris-HCl (pH 7.5), 15 mM MgCl₂, 5 mM β -glycerophosphate, 1 mM EGTA, 0.2 mM Na₂VO₄, 0.2 mM DTT). The wells were resuspended in 20 μ l kinase wash buffer and warmed to 37 °C. Then 20 μ l kinase assay buffer (kinase wash buffer plus 0.4 μ M protein kinase A inhibitor, 4 μ M protein kinase C inhibitor, 4 μ M calmidazolium, 0–25 μ M cold ATP, 1–5 μ Ci [γ -³²P]ATP) was added to the wells, followed by 20 μ l of substrate (40 μ g myelin basic protein for ERK, 10 μ M Aktide (19) for Akt, 3 μ g glutathione S-transferase (GST)-ATF2 (1–109) (20) for JNK1, 10 μ M MK2tide² for MK2, 10 μ g GST-I κ B α (1–62) (21) for IKK) to initiate the reaction. The kinase reactions were allowed to proceed for 15–120 min at 37 °C, then terminated by 60 μ l 75 mM H₃PO₄ or 20 mM EDTA. Exact conditions for each kinase assay are detailed in Table I. For EDTA-terminated reactions, 40 μ l of the terminated reaction was transferred to a phosphocellulose filter plate (Millipore, Bedford, MA) containing 100 μ l 75 mM H₃PO₄ and mixed, whereas H₃PO₄-terminated reactions were added directly to the filter plates. The terminated reaction con-

² I. A. Manke and M. B. Yaffe, manuscript in preparation.

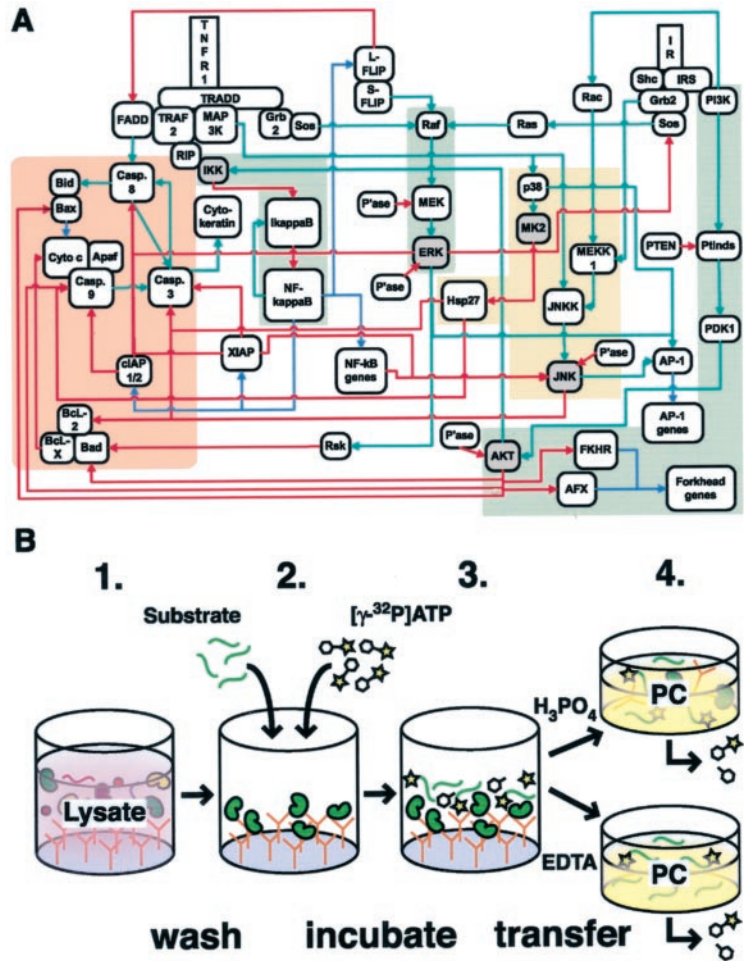
TABLE I
Experimental conditions for the individual *in vitro* kinase assays

Other experimental parameters were maintained as described in "Experimental Procedures."

Kinase	Antibody	Substrate	ATP (μM)	$[\gamma\text{-}^{32}\text{P}]\text{ATP}$ (μCi)	Reaction time (min)	Termination
ERK	Anti-ERK1/2 CT	Myelin basic protein	25	1	60	H_3PO_4
Akt	Anti-Akt PH dom.	Aktide	10	5	30	H_3PO_4
JNK1	Anti-JNK1	GST-ATF2 (1-109)	10	2	60	H_3PO_4
IKK	Anti-IKK α/β	GST-I $\kappa\text{B}\alpha$ (1-62)	0	5	120	EDTA
MK2	Anti-MAPKAP K2	MK2tide	25	2	15	EDTA

FIG. 1. A high-throughput assay of multiple endogenous kinase activities can monitor information flow through critical nodes in a signaling network.

A, generalized network diagram describing pathways activated downstream of TNF- α and insulin: activating interactions (green arrows), inhibitory interactions (red arrows), transcriptional interactions (blue arrows). Gray nodes highlight kinases that are measured by the high-throughput multiplex kinase activity assay. Red regions indicate apoptotic pathways, green regions indicate survival pathways, and orange regions indicate stress pathways that can function to promote or inhibit apoptosis, depending on context. Note the extent of crosstalk in the network. Diagram is not implied to be comprehensive (e.g. location-dependent interactions have been abstracted). B, general schematic of the high-throughput multiplex kinase activity assay format. Lysates are incubated with Protein A or G microtiter wells pre-coated with anti-kinase antibody. After several washes, an appropriate substrate and $[\gamma\text{-}^{32}\text{P}]\text{ATP}$ are added to the plate to initiate an *in vitro* phosphorylation reaction. The reaction is terminated with H_3PO_4 (for Akt and JNK1 assays) or EDTA (for IKK and MK2 assays), and a fraction of the reaction mix is transferred to a PC filter plate and washed to remove free ^{32}P .



tents were vacuum-filtered and washed five times with 75 mM H_3PO_4 and three times with 70% EtOH. The filters were punched into vials and the radioactivity incorporated was measured by liquid scintillation (Cytosint; ICN Pharmaceuticals, Costa Mesa, CA). The results from blank wells, containing only lysis buffer during the immunopurification step, were subtracted to remove nonspecific contributions, with the exception of Akt, where this was not necessary.

Western Blotting—For determination of target capture, assays were stopped before the kinase reaction step and resuspended in 40 μl sample buffer (62.5 mM Tris-HCl (pH 6.8), 2% SDS, 10% glycerol, 100 mM DTT, 0.01% bromphenol blue). Wells were boiled for 5 min, and the samples were resolved on a 10% polyacrylamide gel and transferred to polyvinylidene difluoride (Millipore). Membranes were blocked with 5% nonfat skim milk in 20 mM Tris-HCl (pH 7.5), 137 mM NaCl, 0.1% Tween-20, and probed with the following primary anti-

bodies at 1:1000 dilution: anti-Akt (Upstate Biotechnology), anti-JNK1 (Santa Cruz Biotechnology), anti-MAPKAPK2 (StressGen Biotechnologies, Victoria, British Columbia, Canada), and anti-IKK α/β (Santa Cruz Biotechnology). The membranes were then probed with horseradish peroxidase conjugated anti-mouse or anti-rabbit secondary antibody (Amersham Pharmacia Biotech) at 1:10,000 dilution and visualized by enhanced chemiluminescence (Amersham Pharmacia Biotech) on a FluorS (Bio-Rad) or Kodak Image Station (Perkin Elmer). Bands were selected and quantified according to the manufacturer's recommendations.

Autoradiography—Thirty microliters of the terminated kinase reactions were mixed with 10 μl 4 \times sample buffer and resolved on a 10% polyacrylamide glycine gel for protein substrates or a 16% polyacrylamide tricine gel for peptide substrates (22). The dye front was excised, and the gel exposed overnight to a multisensitive BaFBr:

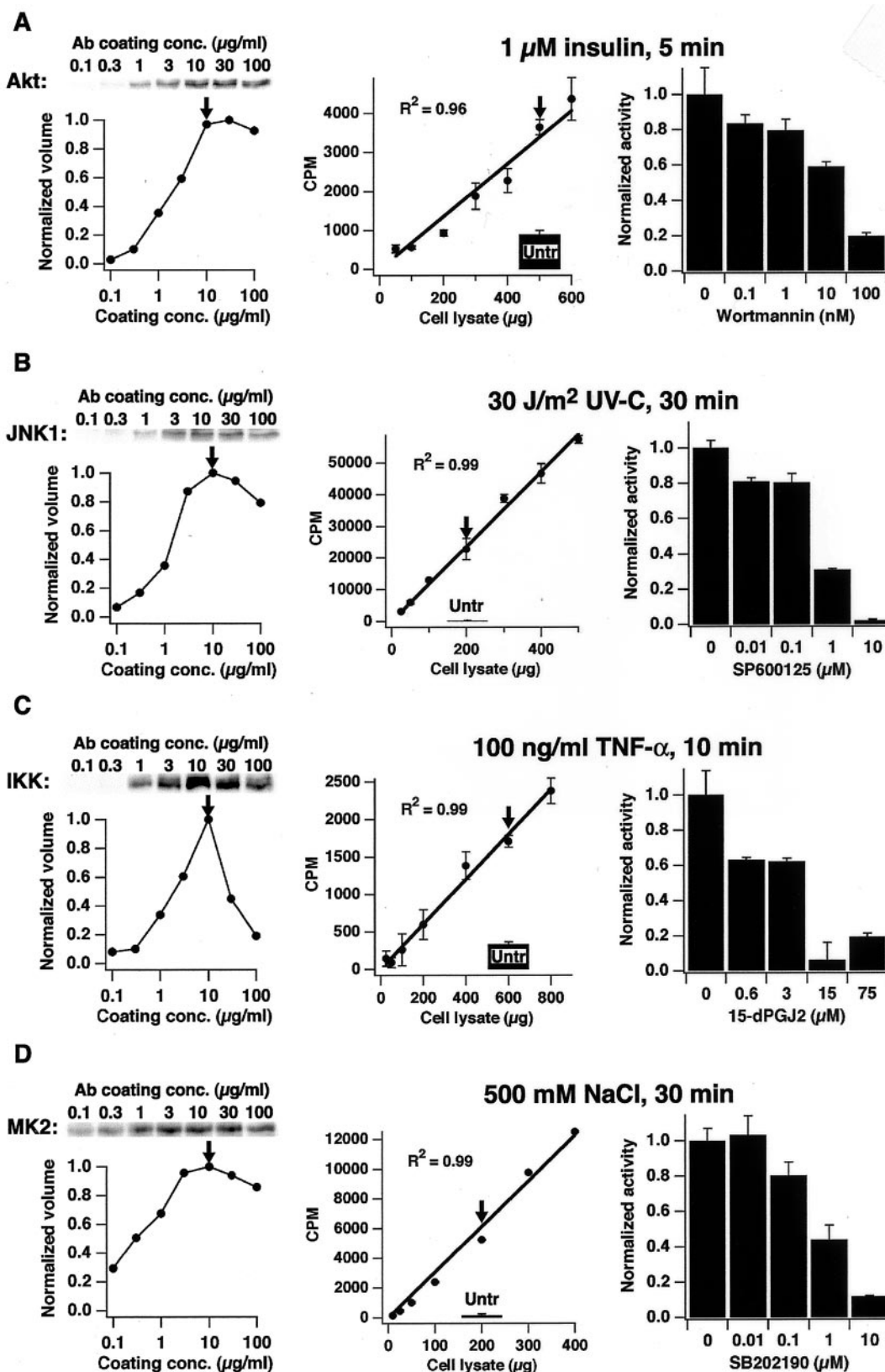


FIG. 2. High-throughput multiplex kinase activity assays are optimally sensitive, quantitatively linear, and specific for the target kinase. *A*, Left panel, Akt was immunopurified from 500 μg of HT-29 lysate on Protein G microtiter plates coated with 50 μl of anti-Akt at various coating concentrations. Plate-bound Akt was analyzed by Western blotting, as described under "Experimental Procedures," and

Eu²⁺ screen (Perkin Elmer). The screen was visualized using a Cyclone Storage Phosphor system (Perkin Elmer).

Cell Imaging—HT-29 cells were seeded in Delta T glass culture dishes (Bioprotech). After 30 h, cells were pretreated with IFN- γ as described, then rinsed and treated with 50 ng/ml TNF- α or 50 ng/ml TNF- α + 100 nM insulin for 18 h. Then 6 μ g/ml Hoechst 33342 (Molecular Probes, Eugene, OR) was added to the medium, and phase and fluorescence images were collected. Cells were then fixed with 100% MeOH and stored at -20 °C overnight. After primary staining with anti-cleaved caspase 3 (Cell Signaling, Beverly, MA) and secondary staining with Alexa 594-conjugated anti-rabbit IgG (Molecular Probes), fluorescence images were collected.

Apoptosis Assays—HT-29 cells were seeded in 96-well plates and sensitized with IFN- γ as described. For inhibitor studies, 20 μ M LY294002 was added to the medium 1 h before or 3 h after cytokine stimulation. During washout experiments, the medium was removed and the wells washed once with PBS. The medium was then replaced with medium conditioned by cells treated with the same cytokine concentrations without inhibitor. After 18 h, cells were rinsed with PBS and trypsinized. The supernatant and rinse were saved and combined with the trypsinized cells to ensure capture of both floating and adherent cells. The cells were washed with PBS, then fixed in 100% MeOH and stored at -20 °C. The fixed cells were stained with a fluorescein-labeled monoclonal antibody against caspase-cleaved cyokeratin (M30; Roche), plus anti-cleaved-caspase-3 (Asp 175; Cell Signaling) with Alexa 647-conjugated anti-rabbit secondary (Molecular Probes), according to the manufacturers' instructions. Cells were washed once after staining, then analyzed by flow cytometry (FACS-calibur; Becton-Dickinson, Mountain View, CA). Cells positive for cleaved cyokeratin, cleaved caspase-3, or both were scored as apoptotic. Three separate biological samples were analyzed for each treatment condition. Percent increased survival was calculated according to the following formula: $[1 - (\% \text{ apoptotic cells in the presence of insulin})/(\% \text{ apoptotic cells in the absence of insulin under the same pretreatment conditions})] \times 100\%$.

RESULTS AND DISCUSSION

High-throughput Kinase Activity Assay Development—The generalized assay format involves four steps, shown in Fig. 1B: i) parallel purification of endogenous kinase from whole cell lysates by immunoprecipitation onto Protein A or G mi-

croter plates that have been precoated with kinase-specific antibodies, ii) low stringency washes to remove nonpurified lysate components, iii) addition of [γ -³²P]ATP and a kinase-specific substrate to initiate an *in vitro* kinase reaction, and iv) termination of the *in vitro* reaction either by H₃PO₄ or EDTA and liquid transfer to a 96-well phosphocellulose (PC) filter plate to isolate phosphoproteins and remove free [γ -³²P]ATP. We developed assays for ERK (3), Akt, JNK1, IKK, and MK2 activity in cell extracts after rigorous optimization and quantitative validation.

To develop the parallel immunopurification step, we experimentally screened multiple commercially available products and identified for each kinase a single, high-affinity antibody that retained enzymatic activity. Coating conditions for each anti-kinase antibody on Protein A/G microtiter plates were individually optimized, revealing that the antibodies maximally bound their intended targets when 50 μ l of 10 μ g/ml antibody was applied to each well (Fig. 2, A–D, left panels), consistent with our estimates of the number of antibody binding sites on the plate surface. Higher coating concentrations of polyclonal antibodies (anti-JNK1, anti-IKK α/β , and anti-MK2) reduced the solid-phase avidity for the kinase and caused a net decrease in purification efficiency (Fig. 2, B–D, left panels). At the optimized coating concentration (Fig. 2, A–D, left panels, arrows), the immunopurification was always linear in the amount of kinase purified over a substantial range of lysate concentrations (Fig. 3, A–D). This demonstrates that the antibody capture step linearly reflects kinase abundance in the lysate.

Next, kinase reaction conditions for each assay were optimized by modifying the following *in vitro* parameters: choice of substrate, concentration of substrate, radioactive-to-non-radioactive ATP ratio, and reaction duration (see "Experimental Procedures"). When an individual kinase was determined to phosphorylate multiple substrates effectively (Fig. 4, A, B, and D and data not shown), the substrate showing the highest

quantified by densitometry of the band intensity to calculate a normalized volume. *Middle panel*, 50–600 μ g of lysate from HT-29 cells treated with 1 μ M insulin for 5 min was measured with the high-throughput Akt activity assay using 10 μ M Aktide as substrate, as described under "Experimental Procedures." The stimulated lysate (arrow) was compared with 500 μ g untreated control lysate (solid bar). *Right panel*, HT-29 cells were pretreated with various concentrations of wortmannin (Sigma) for 1 h then stimulated with 1 μ M insulin for 5 min and lysed. Akt activity was quantified as described under "Experimental Procedures." *B*, Left panel, JNK1 was immunopurified from 200 μ g of HT-29 lysate on Protein A microtiter plates coated with 50 μ l of anti-JNK1 at various coating concentrations and analyzed as described in A. *Middle panel*, 25–500 μ g of lysate from HT-29 cells harvested 30 min after treatment with 30 J/m² UV-C was measured with the high-throughput JNK1 activity assay using 3 μ g GST-ATF2 (1-109) as substrate, as described under "Experimental Procedures." The stimulated lysate (arrow) was compared with 200 μ g untreated control lysate (solid bar). *Right panel*, plate-bound JNK1 from UV-stimulated HT-29 cells was incubated for 10 min with various concentrations of SP600125 (Calbiochem), and JNK1 activity was quantified as described under "Experimental Procedures." *C*, Left panel, IKK was immunopurified from 800 μ g of HT-29 lysate on Protein A microtiter plates coated with 50 μ l of anti-IKK α/β at various coating concentrations and analyzed as described in A. *Middle panel*, 50–800 μ g of lysate from HeLa cells treated with 100 ng/ml TNF- α for 10 min was measured with the high-throughput IKK activity assay using 10 μ g GST-I κ B α (1-62) as substrate, as described under "Experimental Procedures." The stimulated lysate (arrow) was compared with 600 μ g untreated control lysate (solid bar). *Right panel*, plate-bound IKK from TNF-stimulated HeLa cells was incubated for 1 h with various concentrations of 15-deoxy- $\Delta^{12,14}$ -prostaglandin J₂ (15d-PGJ₂; Calbiochem), and IKK activity was quantified as described under "Experimental Procedures." *D*, Left panel, MK2 was immunopurified from 200 μ g of HT-29 lysate on Protein G microtiter plates coated with 50 μ l of anti-MK2 at various coating concentrations and analyzed as described in A. *Middle panel*, 10–400 μ g of lysate from HT-29 cells treated with 500 mM NaCl for 30 min was measured with the high-throughput MK2 activity assay using 10 μ M MK2tide as substrate, as described under "Experimental Procedures." The stimulated lysate (arrow) was compared with 200 μ g untreated control lysate (solid bar). *Right panel*, HT-29 cells were pretreated with various concentrations of SB202190 (Calbiochem) for 1 h then stimulated with 500 mM NaCl for 30 min and lysed. MK2 activity was quantified as described under "Experimental Procedures." All kinase activities are reported as the mean \pm S.E. of triplicate samples (error bars for the MK2 assay were smaller than the size of the marker). Western blots were repeated at least twice with similar results; representative images are shown. Arrows indicate fixed experimental conditions for the adjacent experiment.

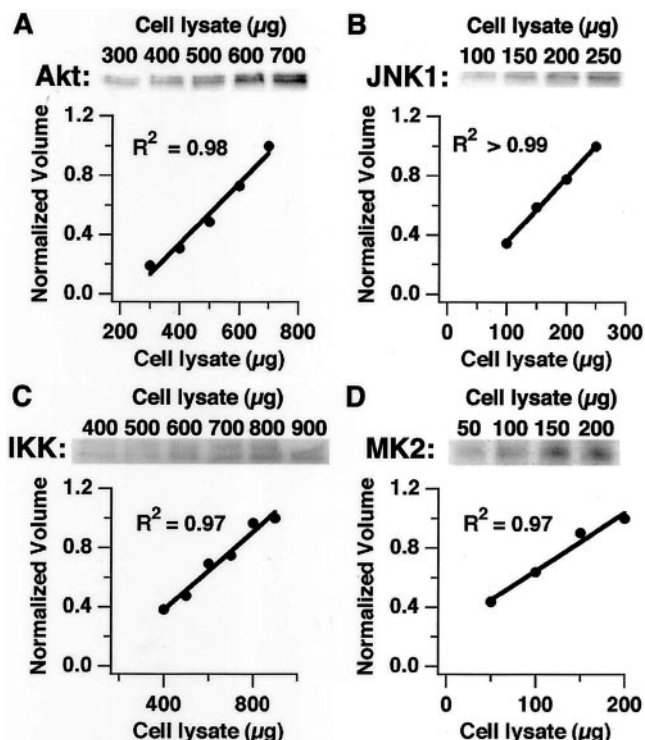


FIG. 3. Purification of endogenous kinases is linear on antibody-coated microtiter plates. A, 300–700 μg of HT-29 lysate was incubated for 3 h on Protein G microtiter plates coated with 10 $\mu\text{g}/\text{ml}$ of anti-Akt. Plate-bound Akt was analyzed by Western blotting, as described under “Experimental Procedures,” and quantified by densitometry of the band intensity to calculate a normalized volume. B, 100–250 μg of HT-29 lysate was incubated for 3 h on Protein A microtiter plates coated with 10 $\mu\text{g}/\text{ml}$ of anti-JNK1 and analyzed as described in A. C, 400–900 μg of HT-29 lysate was incubated overnight on Protein A microtiter plates coated with 10 $\mu\text{g}/\text{ml}$ of anti-IKK α/β and analyzed as described in A. D, 50–200 μg of HT-29 lysate was incubated for 3 h on Protein G microtiter plates coated with 10 $\mu\text{g}/\text{ml}$ of anti-MK2 and analyzed as described in A. Western blots were performed at least twice with similar results; representative images are shown.

specific activity (counts per minute (CPM)/ μmol) was selected to maximize sensitivity. Other reaction parameters, such as buffer composition and reaction temperature, were intentionally kept constant to enable assays of different kinases to be performed in parallel on the same microtiter plate in a single step.

ERK, Akt, and JNK1 assays were terminated by adding an equal volume of 75 mM H_3PO_4 to the microtiter reaction well and transferring the well contents to a parallel 96-well PC filter plate for washing and quantitation. MK2 and IKK assays were terminated by adding an equal volume of 20 mM EDTA to the microtiter reaction well and transferring the contents to the 96-well PC filter plate preacidified with 75 mM H_3PO_4 in each well. SDS-PAGE analysis of the terminated reaction mixtures transferred to the PC filter verified that phosphorylation was only occurring on the added substrate (Fig. 4, A–E). Therefore, individual filters in the wells of the PC plate could be punched out for scintillation counting to accurately quantify kinase

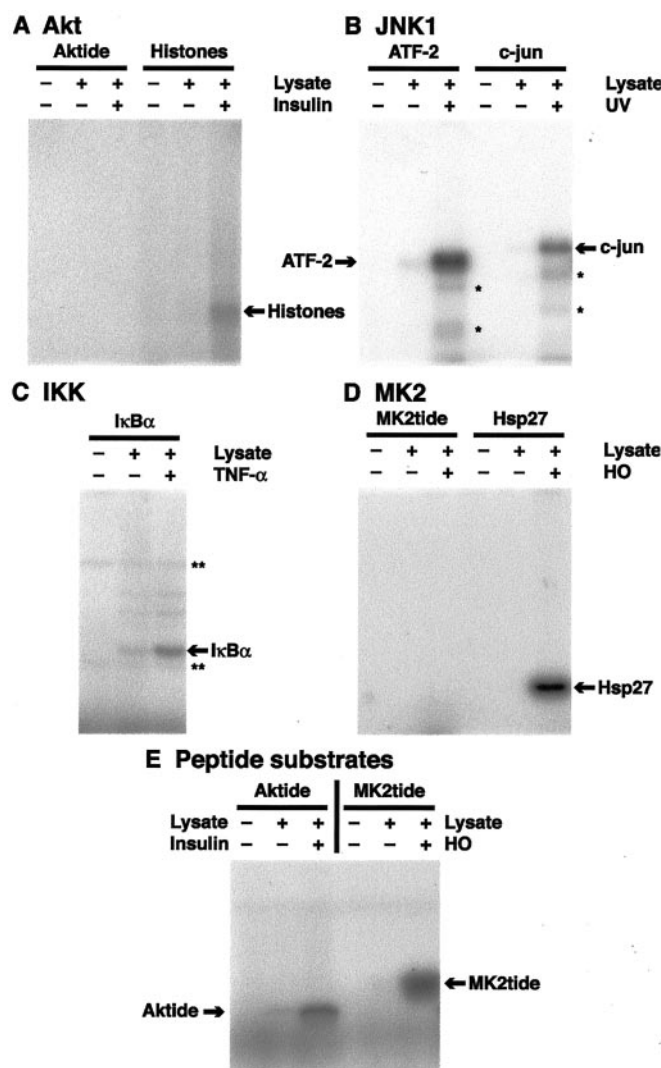


FIG. 4. Terminated *in vitro* reaction products specifically contain the phosphorylated substrate. A, the high-throughput Akt assay, using 10 μM Aktide or 40 μg partially purified histones (Sigma) as substrate, was analyzed by SDS-PAGE and autoradiography after termination of the *in vitro* reaction as described under “Experimental Procedures.” Note that the phosphopeptide has run off the gel and no other phosphorylated bands are evident. B, the high-throughput JNK1 assay, using 3 μg ATF-2 or 2 μg c-jun (Upstate Biotechnology) as substrate, was analyzed as described in A. Single asterisks indicate ^{32}P incorporation into partially cleaved substrates. C, the high-throughput IKK assay, using 10 μg IkB α as substrate, was analyzed as described in A. Double asterisks indicate nonspecific ^{32}P incorporation (note that these bands are of equal intensity in the blank sample, such that background subtraction will remove their contribution). D, the high-throughput MK2 assay, using 10 μM MK2tide or 5 μg Hsp27 (Upstate Biotechnology) as substrate, was analyzed as described in A. Note that the phosphopeptide has run off the gel and no other phosphorylated bands are evident. E, the peptide substrates (10 μM Aktide for the Akt assay and 10 μM MK2tide for the MK2 assay) were analyzed on a 16% tricine-polyacrylamide gel and autoradiographed after termination of the *in vitro* reaction as described under “Experimental Procedures.” The migration position of a 5-kDa marker is indicated.

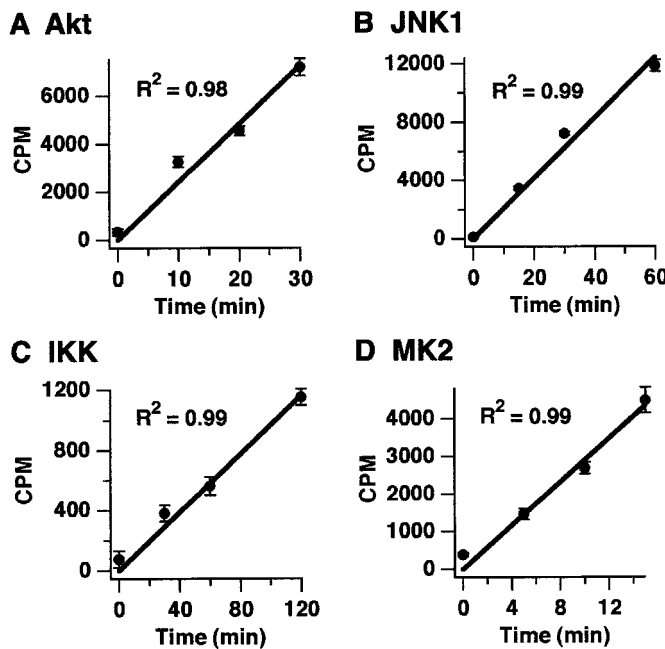


FIG. 5. Kinetics of the *in vitro* kinase reactions are linear with time. Assays were incubated with fixed amounts of HT-29 or HeLa lysates treated with known activators of the pathway of interest (for details, see Fig. 2, A–D). *In vitro* reactions were allowed to proceed for the indicated times and analyzed as described under “Experimental Procedures.” A, Akt assay kinetics with Akt from 500 μg of HT-29 lysate. B, JNK1 assay kinetics with JNK1 from 200 μg of HT-29 lysate. C, IKK assay kinetics with IKK from 800 μg of HeLa lysate. D, MK2 assay kinetics with MK2 from 200 μg of HT-29 lysate.

activity, eliminating the low-throughput, SDS-PAGE-and-autoradiography step required in classical immune complex kinase assays.

To investigate the sensitivity, dynamic range, and linearity of these assays, HT-29 and HeLa cells were treated with known activators of each kinase, and the kinase activities (CPM on the PC filter) measured as a function of different dilutions of the activated lysates (Fig. 2, A–D, middle panels). The ^{32}P incorporation was linear over at least an order of magnitude in activity, and the absolute sensitivities of the assays were always below 200 μg , with some assays capable of measuring activity from as little as 10–25 μg of total lysate. This result is comparable to, or better than, existing assays that usually require several hundred micrograms of lysate for analysis (23–25). The aggregate sensitivity of the format was more than sufficient to measure ERK, Akt, JNK1, MK2, and IKK activity simultaneously from a single 10-cm plate of HT-29 cells.

The signal-to-noise and reproducibility characteristics for each kinase assay were examined by selecting a single concentration in the middle of the dynamic range of each assay (Fig. 2, A–D, middle panels, arrows) and comparing the kinase activities between lysates from stimulated and unstimulated cells. For each agonist, this revealed a relative activation of each endogenous kinase that was comparable in magnitude

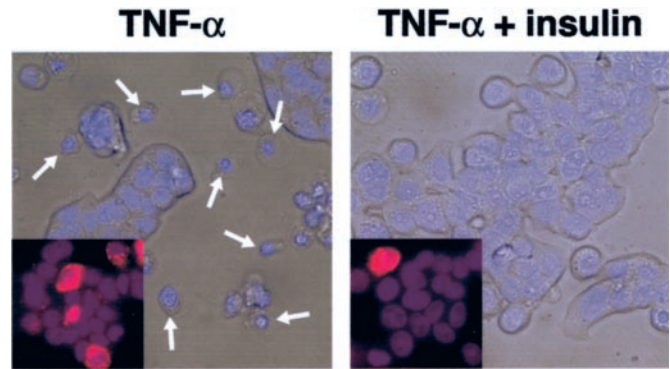


FIG. 6. IFN-sensitized HT-29 cells undergo programmed cell death in response to $\text{TNF-}\alpha$ and can be rescued by cotreatment with insulin. Main panels, phase contrast images of HT-29 cells treated with 100 ng/ml $\text{TNF-}\alpha$ alone (left) and both 100 ng/ml $\text{TNF-}\alpha$ + 100 nM insulin (right) as described under “Experimental Procedures.” Note the increased number of shrunken cells with condensed nuclei in cells treated with $\text{TNF-}\alpha$ alone (arrows). Insets, indirect immunofluorescence images of cleaved caspase 3 (red) in HT-29 cells treated with 100 ng/ml $\text{TNF-}\alpha$ alone (left) and both 100 ng/ml $\text{TNF-}\alpha$ + 100 nM insulin (right). Note the increased number of cleaved caspase 3-positive cells in the $\text{TNF-}\alpha$ alone image. Hoechst 33342 (blue) is overlaid in all images to show nuclei.

to that reported in the literature, with intra-assay coefficients of variation always $\leq 10\%$. Thus, the assays clearly reflected activation of the endogenous pathways, and the end point measures of activity were highly sensitive and reproducible.

In order for these assays to reflect information flow through the signaling network accurately, it was crucial to confirm that our end point CPM measurement linearly reflected the kinase activity in the lysate. Therefore, the kinetics of the *in vitro* reaction were examined in detail at a selecting fixed lysate concentration within the linear range (Fig. 2, A–D, middle panels, arrows). As shown in Fig. 5, A–D, each phosphorylation reaction displayed linear kinetics up to the time of termination, suggesting that neither the $[\gamma\text{-}^{32}\text{P}]\text{ATP}$ nor the substrate was significantly depleted over the course of the reaction. Thus, the linearity at every step in the assay procedure (kinase capture, *in vitro* reaction kinetics, and end point CPM measurement) strongly suggests that these assays are a linear reflection of endogenous kinase activity *in vivo*.

As a final confirmation of assay specificity, we examined the effect of various small molecule inhibitors that have been reported to be specific for each of the measured kinases or the directly upstream kinase (26–29). At a fixed lysate concentration (Fig. 2, A–D, middle panels, arrows), a dose-dependent decrease in the measured activity (Fig. 2, A–D, right panels) was observed, consistent with the reported IC_{50} values for the target kinase. Taken together with the redundant antibody-kinase and kinase-substrate specificity inherent to the measurement format, these results strongly suggest that the assays specifically quantify the endogenous activity of the intended kinase. We conclude that the high-throughput

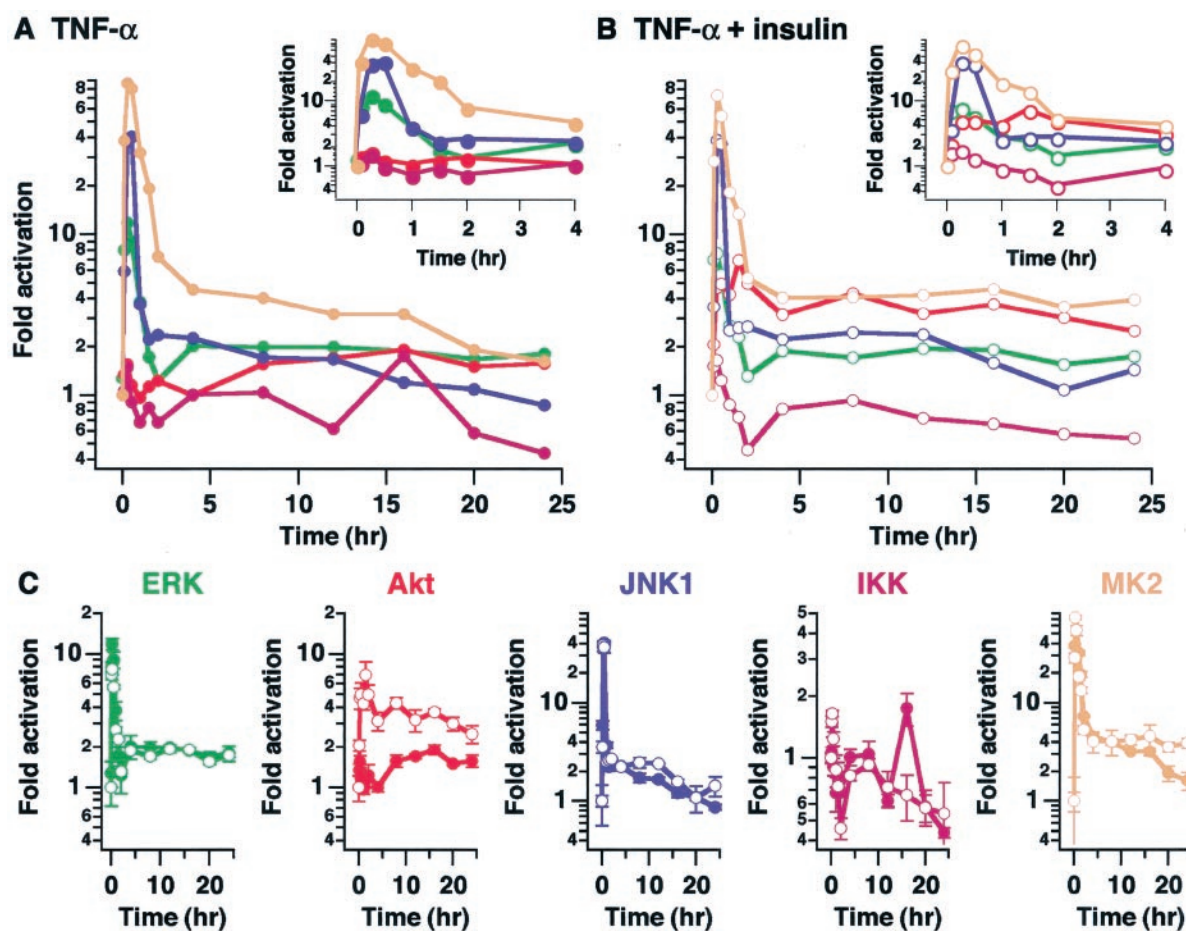


FIG. 7. **TNF- α and TNF- α + insulin treatments elicit quantitatively distinct signaling patterns in HT-29 cells.** Endogenous ERK (green), Akt (red), JNK1 (blue), IKK (purple), and MK2 (orange) activities in HT-29 cells in response to: A, 50 ng/ml TNF- α (filled circles) and B, 50 ng/ml TNF- α + 100 nM insulin (open circles). Lysates were generated at 0, 5, 15, 30, 60, 90 min and 2, 4, 8, 12, 16, 20, 24 h, then measured for kinase activity with the high-throughput multiplex kinase assay. Results are plotted as the mean fold activation of three independent cell extracts. Error bars are omitted for clarity, but are shown in panel C. C, comparison of ERK, Akt, JNK1, IKK and MK2 activities in response to TNF- α (filled circles) and TNF- α + insulin (open circles) from A and B, plotted as mean fold activation \pm S.E. of triplicate samples.

multiplex assays provide reliable, quantitative measurements that are directly reflective of specific protein kinase activities in cell extracts.

Application to an In Vitro Model of Sepsis-induced Colon Epithelial Apoptosis—HT-29 cells are a human colon carcinoma cell line that die in response to TNF- α , following sensitization with interferon gamma (IFN- γ) (30). We confirmed that TNF-treated HT-29 cells exhibit many features of apoptosis, such as cell shrinkage, membrane blebbing, nuclear condensation, and caspase 3 activation (Fig. 6, left). Intriguingly, we found that TNF-induced cell death can be reduced by \sim 30% if HT-29 cells are costimulated with insulin (Fig. 6, right), in agreement with previous reports (31). Given the importance of proinflammatory cytokines, such as TNF- α and IFN- γ , in sepsis (4) and the emerging role of insulin as a therapeutic for critically ill patients (15), we considered HT-29 cells as an appropriate model system for exploring the signaling network dynamics activated by TNF- α and TNF- α + insulin in relation

to a relevant cell phenotype: colon epithelial cell death, as observed during the onset of sepsis (6).

IFN-sensitized HT-29 cells were treated with 50 ng/ml TNF- α , in the presence or absence of 100 nM insulin cotreatment, and triplicate lysates were prepared at 13 time points over 24 h. Because much of the signaling induced by these cues occurs shortly after cytokine addition, time points were more densely sampled in the first 4 h (Fig. 7, A and B, inset). From these cell extracts, quantitative measurements of ERK, Akt, JNK1, MK2, and IKK kinase activity were performed using the high-throughput multiplex kinase activity assays (Fig. 7, A and B). To our knowledge, this set of time courses, consisting of over 400 independent activity measurements, represents the most comprehensive, rigorously quantitative study of functional signaling dynamics performed to date. To achieve this depth of quantitative, replicated network sampling by traditional techniques would have been extraordinarily laborious and technically impractical.

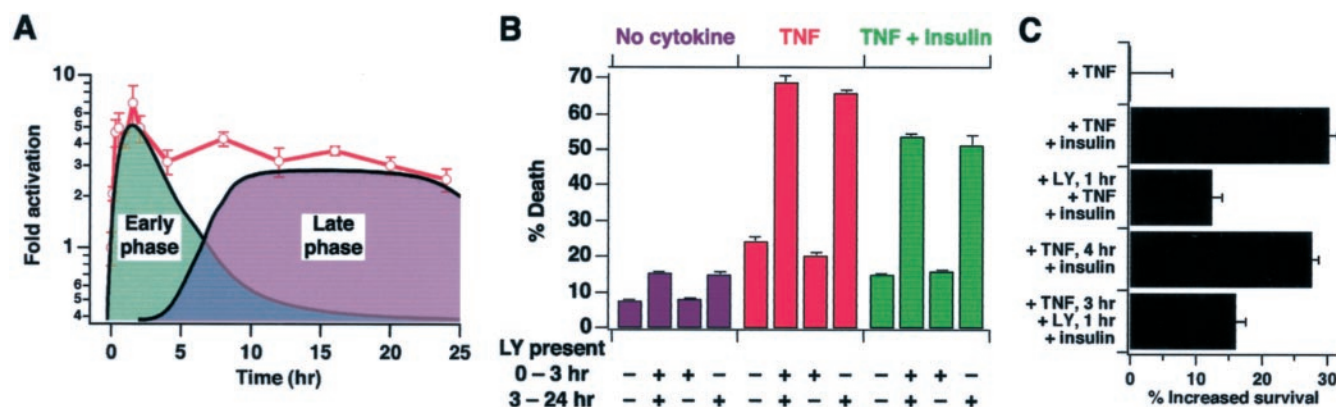


FIG. 8. Insulin elevates two phases of Akt activity, and the late-phase of Akt activity provides a critical anti-apoptotic signal in HT-29 cells. A, hypothetical two-phase contribution to the sustained Akt activity that was observed in the presence of insulin (Fig. 7, B and C). B, HT-29 cell death in response to no cytokines (■), 50 ng/ml TNF- α (■), or 50 ng/ml TNF- α + 100 nM insulin (■) in the presence of 20 μ M LY294002 (LY) at the indicated times. Cells were stained for cleaved cytokeratin and cleaved caspase 3 and analyzed by flow cytometry as described under "Experimental Procedures." Values represent the percentage of apoptotic cells \pm S.E. of triplicate samples. C, HT-29 cell survival in response to timed combinations of 50 ng/ml TNF- α , 100 nM insulin, and 20 μ M LY294002. Values represent the percentage of increased survival \pm S.E. of triplicate samples, computed as described under "Experimental Procedures." The carrier (0.1% DMSO) was kept constant for control experiments.

Furthermore, to deconstruct the effects of insulin therapy on the signaling network in the context of TNF- α signaling, a pairwise comparison was performed for each kinase under TNF- α with and without insulin costimulation. As shown in Fig. 7C, the dynamics of activation of some pathways, such as the ERK pathway (Fig. 7C, green), were essentially superimposable. Thus insulin does not appear to influence activation of the ERK pathway by TNF- α under these conditions. Other TNF-induced kinase activities were affected by insulin in a time-dependent manner. JNK1 activity, for example, was larger at intermediate times (8–16 h), while IKK activity was smaller at 16 h, and MK2 activity was larger at late times (16–24 h). Although potentially important, these transient signaling differences did not clearly reflect the insulin-induced survival phenotype observed at the cellular level (Fig. 6).

Late-phase Akt Activity as a Critical Pro-survival Signal—In contrast to the subtle influences of insulin on ERK, JNK1, IKK, and MK2 signaling, it was readily apparent that insulin dramatically augmented Akt activity, inducing a rapid increase within 5 min and sustaining activation for 24 h, whereas with TNF- α alone, the Akt response was much smaller in magnitude (Fig. 7C, red). In addition to these quantitative differences, we noted that the dynamic TNF-induced Akt response was also qualitatively different without insulin, in that the course of activation was clearly biphasic, with a brief initial peak, followed by a small (*i.e.* 2-fold), sustained increase in activity after 4 h. If these data had not been rigorously quantitative, or had the signaling network not been sampled frequently in time, this increase in activity would likely have been missed. By virtue of the high-throughput activity assays, however, it was clear that Akt activity after 4 h was significantly up-regulated in comparison to baseline activity ($p < 0.05$ for all times after 4 h, Student's *t* test).

These findings suggested that a significant component of the insulin-induced anti-apoptotic effect was mediated by the high sustained Akt activity, and that this activity profile was derived from the superposition of an early, elevated phase of activity that was transient with a late, elevated phase of activity that was sustained (Fig. 8A). Conversely, in cells treated with TNF- α alone, these two phases were reduced in intensity and separated in time. Because Akt is thought to provide strong pro-survival signals (10), we hypothesized that one or both of these temporal components of Akt activation were involved in controlling the phenotypic response of HT-29 cells to TNF- α and insulin.

To investigate this, we used a reversible, selective inhibitor (LY294002 (32)) of phosphatidylinositol 3-kinase (PI 3-K), an upstream activator of Akt. LY294002 was added or removed at critical times to eliminate the early phase of Akt activity, the late phase of Akt activity, or both, and apoptosis was quantified by flow cytometry with an anti-cleaved caspase 3 antibody and the M30 antibody (33) against caspase-cleaved cytokeratin. We have found this double stain to be the most sensitive, quantitatively reproducible measure of apoptosis in HT-29 cells.³

When LY294002 was added 1 h before cytokine addition and tonically maintained to block Akt activity over the entire time course, a dramatic increase in TNF-induced cell death was observed (Fig. 8B, red). Surprisingly, if LY294002 was present only for the first 3 h of TNF- α addition, thus permitting only the late phase of Akt activity, there was no increased cell death relative to treatments without inhibitor. In contrast, when LY294002 was first added at 3 h after cytokine addition to selectively abolish late-phase Akt activity, we observed an increase in cell death equivalent to that observed when the

³ J. G. Albeck, unpublished observations.

inhibitor was present for the entire 24 h. An identical pattern was observed in response to TNF- α + insulin (Fig. 8B, green), whereas LY294002 had only a small effect on basal apoptosis (Fig. 8B, blue). These data suggest that late-phase Akt activation is necessary to restrain the percentage of cells undergoing programmed cell death in response to TNF- α in the presence or absence of insulin.

The importance of late Akt activity in controlling TNF-induced cell death, in conjunction with the strong, sustained late Akt activation in the presence of insulin, led to the hypothesis that the insulin-induced increase in cell survival was due, in part, to this increase in late-phase Akt signaling. If true, then addition of insulin up to 4 h after the pro-death stimulus should elicit an equivalent reduction in the extent of TNF-induced apoptosis. Indeed, this was observed; the delayed addition of insulin 4 h following TNF- α addition resulted in the same increase in HT-29 cell survival as observed when insulin was added simultaneously with TNF- α (Fig. 8C). Moreover, pretreatment with LY294002 1 h before insulin addition significantly reduced the survival response, regardless whether insulin was added simultaneously or 4 h after TNF- α treatment (Fig. 8C).

These experiments strongly implicate late-phase signaling, along a PI 3-K-dependent/Akt pathway, as a critical pro-survival mechanism of insulin in colon epithelia. Excessive apoptosis in the gut leads to disruption of the epithelial permeability barrier (7) that drives many of the complications of the septic state (8). Our results provide a partial molecular explanation why intensive insulin therapy, administered hours after the initial septic insult, is capable of reducing sepsis-induced apoptosis of gastrointestinal epithelia and improving the prognostic outcome in critically ill patients.

We stress that it was the ability to robustly sample the dynamics of multiple nodes in the signaling network with the high-throughput multiplex kinase assay format described in this paper that enabled the identification of Akt as an important signal for modulating cell response. Other insulin-induced, PI 3-K independent pathways must also attenuate the TNF-induced apoptotic phenotype in HT-29 cells, because inhibition of PI 3-K/Akt by LY294002 did not completely abrogate the rescue response of insulin (Fig. 8C). Thus, i) there may exist additional response-determining pathways that our measurements did not capture, or ii) the subtle, time-dependent quantitative differences we measured in the JNK1, IKK, and MK2 pathways (Fig. 7C) may modulate phenotypic response. We are currently investigating both these possibilities.

The current knowledge of intracellular signal transduction is staggeringly complex. To identify network-level properties that affect cell function, it will be necessary to mathematically model the dynamic, multivariate characteristics of signaling proteins within cells (34). For such models to be realized, quantitative experimental techniques that are both high-throughput and multiplex are needed. The kinase activity assay format presented here represents a first step in this di-

rection. The 96-well, microtiter format is highly versatile, in that it is amenable to scale-up and automated liquid handling, yet tractable for individual scientists and more moderate studies. Importantly, these assays possess linearity, reproducibility, specificity, and sensitivity characteristics as good as, or better than, the corresponding low-throughput technique. We anticipate that these functional assays will complement existing proteomic approaches (2) and find broad applicability toward biological and clinical problems involving signal transduction and human disease.

Acknowledgments—We thank Isaac Manke for providing the MK2tide sequence ahead of publication, as well as Roger Davis and Warner Greene for providing various plasmids.

* This work was supported by the Defense Advanced Research Planning Agency Bio-Info-Micro Program, the National Institute of General Medical Sciences Cell Migration Consortium (to D. A. L.), and National Institutes of Health Grant GM59281 (to M. B. Y.). Additional financial support was provided by the Whitaker Foundation (to K. A. J.). The costs of publication of this article were defrayed in part by the payment of page charges. This article must therefore be hereby marked "advertisement" in accordance with 18 U.S.C. Section 1734 solely to indicate this fact.

|| To whom correspondence should be addressed: Center for Cancer Research, Massachusetts Institute of Technology, 77 Massachusetts Ave. E18-580, Cambridge, MA 02139. Tel.: 617-452-2103, Fax: 617-452-4978; E-mail: myaffe@mit.edu.

REFERENCES

1. Nguyen, A., and Yaffe, M. B. (2003) Proteomics and systems biology approaches to signal transduction in sepsis. *Crit. Care Med.* **31**, S1–S6
2. Tyers, M., and Mann, M. (2003) From genomics to proteomics. *Nature* **422**, 193–197
3. Asthagiri, A. R., Horwitz, A. F., and Lauffenburger, D. A. (1999) A rapid and sensitive quantitative kinase activity assay using a convenient 96-well format. *Anal. Biochem.* **269**, 342–347
4. Hotchkiss, R. S., and Karl, I. E. (2003) The pathophysiology and treatment of sepsis. *N. Engl. J. Med.* **348**, 138–150
5. Strassheim, D., Park, J. S., and Abraham, E. (2002) Sepsis: Current concepts in intracellular signaling. *Int. J. Biochem. Cell Biol.* **34**, 1527–1533
6. Hotchkiss, R. S., Schmieg, R. E., Jr., Swanson, P. E., Freeman, B. D., Tinsley, K. W., Cobb, J. P., Karl, I. E., and Buchman, T. G. (2000) Rapid onset of intestinal epithelial and lymphocyte apoptotic cell death in patients with trauma and shock. *Crit. Care Med.* **28**, 3207–3217
7. Bojarski, C., Bendfeldt, K., Gitter, A. H., Mankertz, J., Fromm, M., Wagner, S., Riecken, E. O., and Schulzke, J. D. (2000) Apoptosis and intestinal barrier function. *Ann. N. Y. Acad. Sci.* **915**, 270–274
8. Wattanasirichaigoon, S., Menconi, M. J., Delude, R. L., and Fink, M. P. (1999) Effect of mesenteric ischemia and reperfusion or hemorrhagic shock on intestinal mucosal permeability and ATP content in rats. *Shock* **12**, 127–133
9. Hatherill, M., Tibby, S. M., Turner, C., Ratnavel, N., and Murdoch, I. A. (2000) Procalcitonin and cytokine levels: relationship to organ failure and mortality in pediatric septic shock. *Crit. Care Med.* **28**, 2591–2594
10. Lawlor, M. A., and Alessi, D. R. (2001) PKB/Akt: a key mediator of cell proliferation, survival and insulin responses? *J. Cell Sci.* **114**, 2903–2910
11. Davis, R. J. (2000) Signal transduction by the JNK group of MAP kinases. *Cell* **103**, 239–252
12. Karin, M., and Ben-Neriah, Y. (2000) Phosphorylation meets ubiquitination: The control of NF- κ B activity. *Annu. Rev. Immunol.* **18**, 621–663
13. Stokoe, D., Engel, K., Campbell, D. G., Cohen, P., and Gaestel, M. (1992) Identification of MAPKAP kinase 2 as a major enzyme responsible for the phosphorylation of the small mammalian heat shock proteins. *FEBS Lett.* **313**, 307–313
14. Fisher, C. J., Jr., Agosti, J. M., Opal, S. M., Lowry, S. F., Balk, R. A., Sadoff,

- J. C., Abraham, E., Schein, R. M., and Benjamin, E. (1996) Treatment of septic shock with the tumor necrosis factor receptor:Fc fusion protein. The Soluble TNF Receptor Sepsis Study Group. *N. Engl. J. Med.* **334**, 1697–1702
15. van den Berghe, G., Wouters, P., Weekers, F., Verwaest, C., Bruyninckx, F., Schetz, M., Vlasselaers, D., Ferdinande, P., Lauwers, P., and Bouillon, R. (2001) Intensive insulin therapy in the critically ill patients. *N. Engl. J. Med.* **345**, 1359–1367
16. Van den Berghe, G., Wouters, P. J., Bouillon, R., Weekers, F., Verwaest, C., Schetz, M., Vlasselaers, D., Ferdinande, P., and Lauwers, P. (2003) Outcome benefit of intensive insulin therapy in the critically ill: Insulin dose versus glycemic control. *Crit. Care Med.* **31**, 359–366
17. Hirsch, I. B., and Coviello, A. (2002) Intensive insulin therapy in critically ill patients. *N. Engl. J. Med.* **346**, 1586–1588
18. Hansen, T. K., Thiel, S., Wouters, P. J., Christiansen, J. S., and Van den Berghe, G. (2003) Intensive insulin therapy exerts antiinflammatory effects in critically ill patients and counteracts the adverse effect of low mannose-binding lectin levels. *J. Clin. Endocrinol. Metab.* **88**, 1082–1088
19. Obata, T., Yaffe, M. B., Leparo, G. G., Piro, E. T., Maegawa, H., Kashiwagi, A., Kikkawa, R., and Cantley, L. C. (2000) Peptide and protein library screening defines optimal substrate motifs for AKT/PKB. *J. Biol. Chem.* **275**, 36108–36115
20. Gupta, S., Campbell, D., Derijard, B., and Davis, R. J. (1995) Transcription factor ATF2 regulation by the JNK signal transduction pathway. *Science* **267**, 389–393
21. Geleziunas, R., Ferrell, S., Lin, X., Mu, Y., Cunningham, E. T., Jr., Grant, M., Connelly, M. A., Hambor, J. E., Marcu, K. B., and Greene, W. C. (1998) Human T-cell leukemia virus type 1 Tax induction of NF-kappaB involves activation of the IkappaB kinase alpha (IKKalpha) and IKKbeta cellular kinases. *Mol. Cell. Biol.* **18**, 5157–5165
22. Judd, R. C. (1994) Electrophoresis of peptides, in *Methods in Molecular Biology* (Walker, J. M., ed.) p. 32, Humana Press, Totowa, NJ
23. Whitmarsh, A. J., and Davis, R. J. (2001) Analyzing JNK and p38 mitogen-activated protein kinase activity. *Methods Enzymol.* **332**, 319–336
24. Hill, M. M., and Hemmings, B. A. (2002) Analysis of protein kinase B/Akt. *Methods Enzymol.* **345**, 448–463
25. Kupfer, R., and Scheinman, R. I. (2002) Measurement of IKK activity in primary rat T cells: rapid activation and inactivation. *J. Immunol. Methods.* **266**, 155–164
26. Arcaro, A., and Wymann, M. P. (1993) Wortmannin is a potent phosphatidylinositol 3-kinase inhibitor: the role of phosphatidylinositol 3, 4, 5-trisphosphate in neutrophil responses. *Biochem. J.* **296** (Pt 2), 297–301
27. Bennett, B. L., Sasaki, D. T., Murray, B. W., O'Leary, E. C., Sakata, S. T., Xu, W., Leisten, J. C., Motiwala, A., Pierce, S., Satoh, Y., Bhagwat, S. S., Manning, A. M., and Anderson, D. W. (2001) SP600125, an anthranyrazolone inhibitor of Jun N-terminal kinase. *Proc. Natl. Acad. Sci. U. S. A.* **98**, 13681–13686
28. Rossi, A., Kapahi, P., Natoli, G., Takahashi, T., Chen, Y., Karin, M., and Santoro, M. G. (2000) Anti-inflammatory cyclopentenone prostaglandins are direct inhibitors of IkappaB kinase. *Nature* **403**, 103–108
29. Lee, J. C., Laydon, J. T., McDonnell, P. C., Gallagher, T. F., Kumar, S., Green, D., McNulty, D., Blumenthal, M. J., Heys, J. R., Landvatter, S. W., Strickler, J. E., McLaughlin, M. M., Siemens, J. R., Fisher, S. M., Livi, G. P., White, J. R., Adams, J. L., and Young, P. R. (1994) A protein kinase involved in the regulation of inflammatory cytokine biosynthesis. *Nature* **372**, 739–746
30. Abreu-Martin, M. T., Vidrich, A., Lynch, D. H., and Targan, S. R. (1995) Divergent induction of apoptosis and IL-8 secretion in HT-29 cells in response to TNF-alpha and ligation of Fas antigen. *J. Immunol.* **155**, 4147–4154
31. Remacle-Bonnet, M. M., Garrouste, F. L., Heller, S., Andre, F., Marvaldi, J. L., and Pommier, G. J. (2000) Insulin-like growth factor-I protects colon cancer cells from death factor-induced apoptosis by potentiating tumor necrosis factor alpha-induced mitogen-activated protein kinase and nuclear factor kappaB signaling pathways. *Cancer Res.* **60**, 2007–2017
32. Vlahos, C. J., Matter, W. F., Hui, K. Y., and Brown, R. F. (1994) A specific inhibitor of phosphatidylinositol 3-kinase, 2-(4-morpholinyl)-8-phenyl-4H-1-benzopyran-4-one (LY294002). *J. Biol. Chem.* **269**, 5241–5248
33. Leers, M. P., Kolgen, W., Bjorklund, V., Bergman, T., Tribbick, G., Persson, B., Bjorklund, P., Ramaekers, F. C., Bjorklund, B., Nap, M., Jornvall, H., and Schutte, B. (1999) Immunocytochemical detection and mapping of a cytokeratin 18 neo-epitope exposed during early apoptosis. *J. Pathol.* **187**, 567–572
34. Asthagiri, A. R., and Lauffenburger, D. A. (2000) Bioengineering models of cell signaling. *Annu. Rev. Biomed. Eng.* **2**, 31–53